

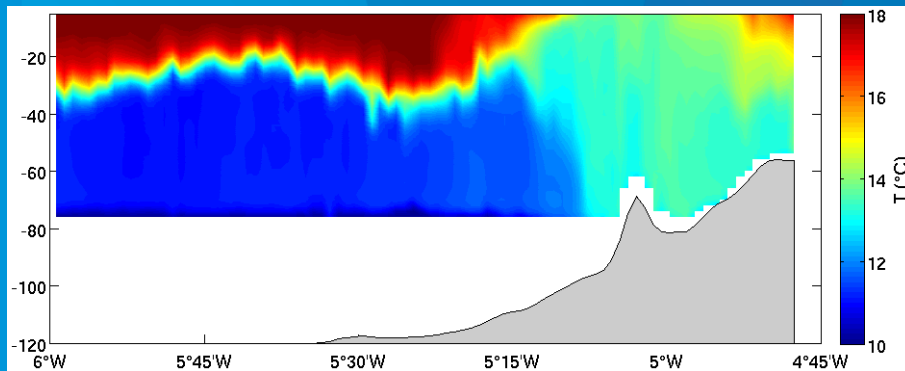
Dynamics of the Ushant front in the Iroise sea

Tanguy Szekely, Louis Marié, Yves Morel

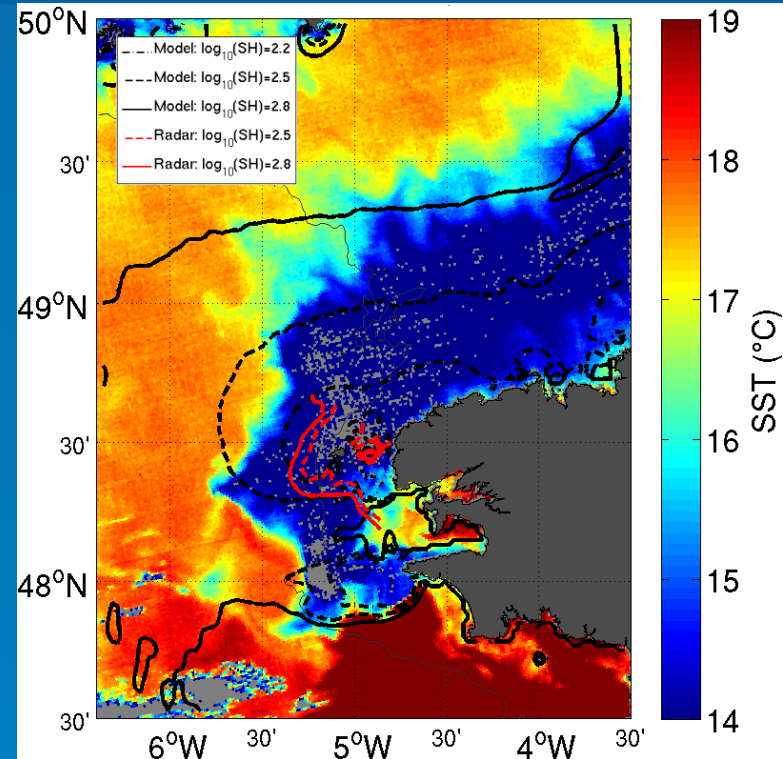


Observations of the Ushant tidal front

- Tidal fronts are coastal density fronts
 - Homogeneous waters, mixed by tides
 - Stratified waters



Temperature section of the Ushant front, along the 48°16' N radial. (FROMVAR cruise, July 2010)

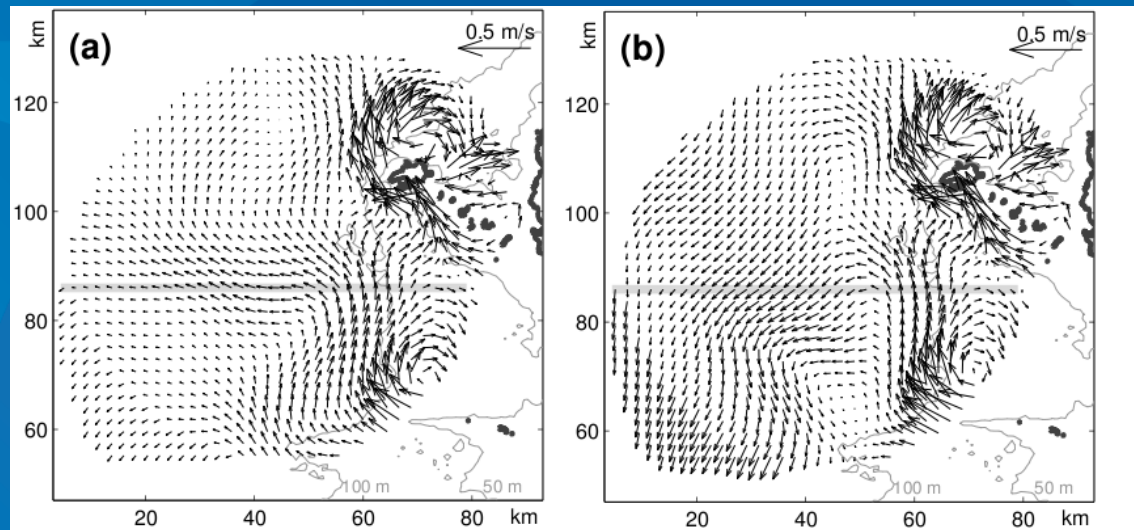


Simpson-Hunter criterion computed by tide model (black) and Radar observations (red)

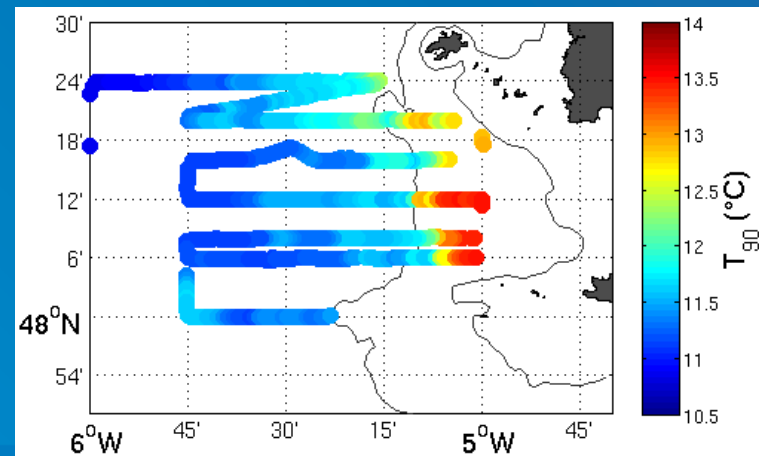
$$SH = \frac{h}{U^3}$$

Observations of the Ushant tidal front

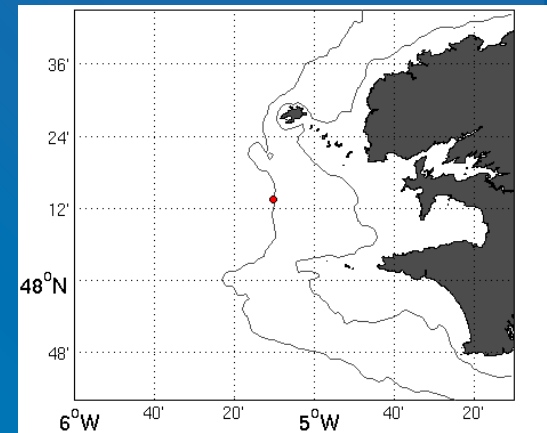
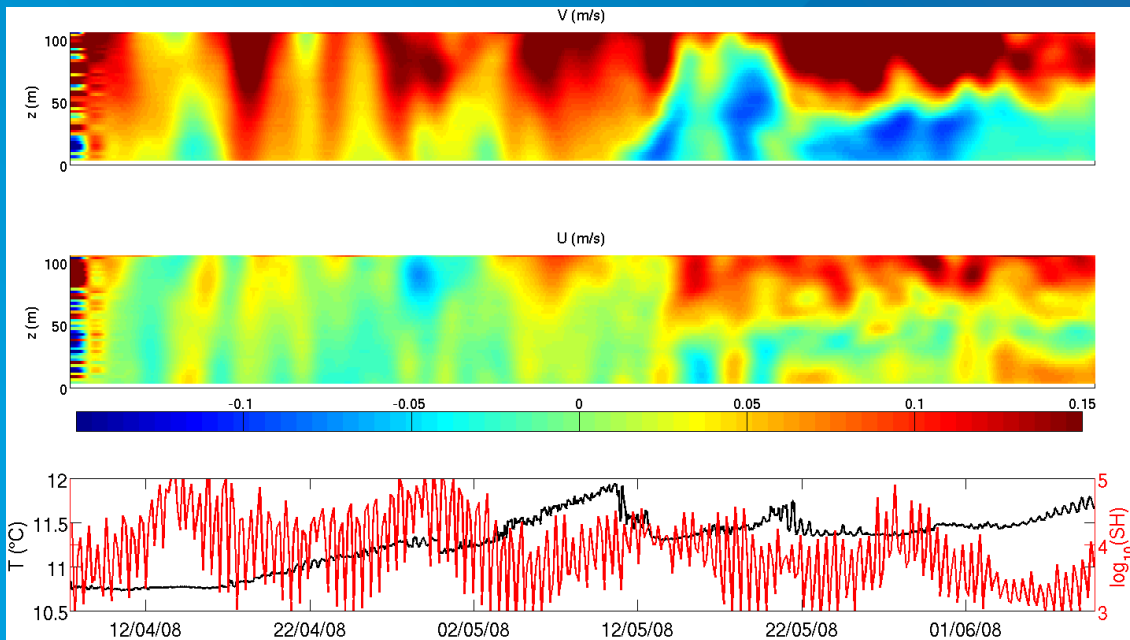
Residual currents measured by HF radars in April (a) and September 2007 (b)
(Sentchev et al. 2010)



Mean temperature between -70 and -80 meters measured during the FROMVAR cruise, in August 2010.



Observations of the Ushant tidal front

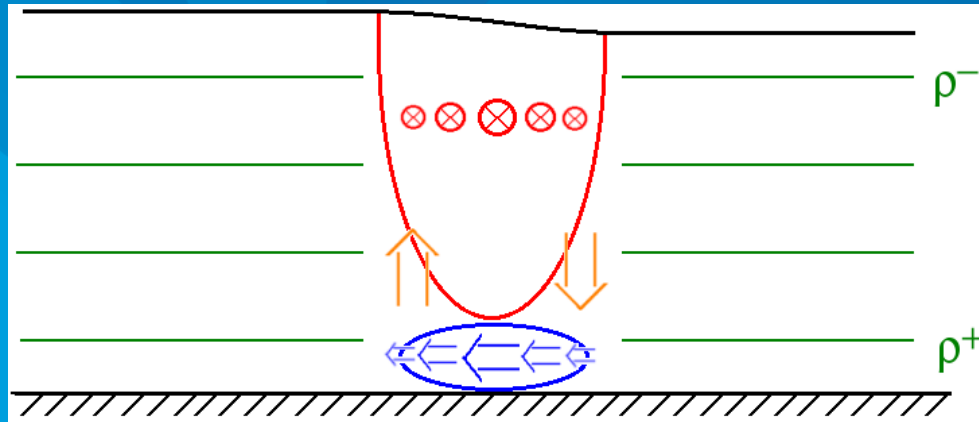


Circulation measured by an ADCP mooring, filtered from tidal motion (1 and 2).
Temperature at 102m depth and Simpson-Hunter criterion.

The residual jet is almost barotropic.

Frontogenetic mechanism

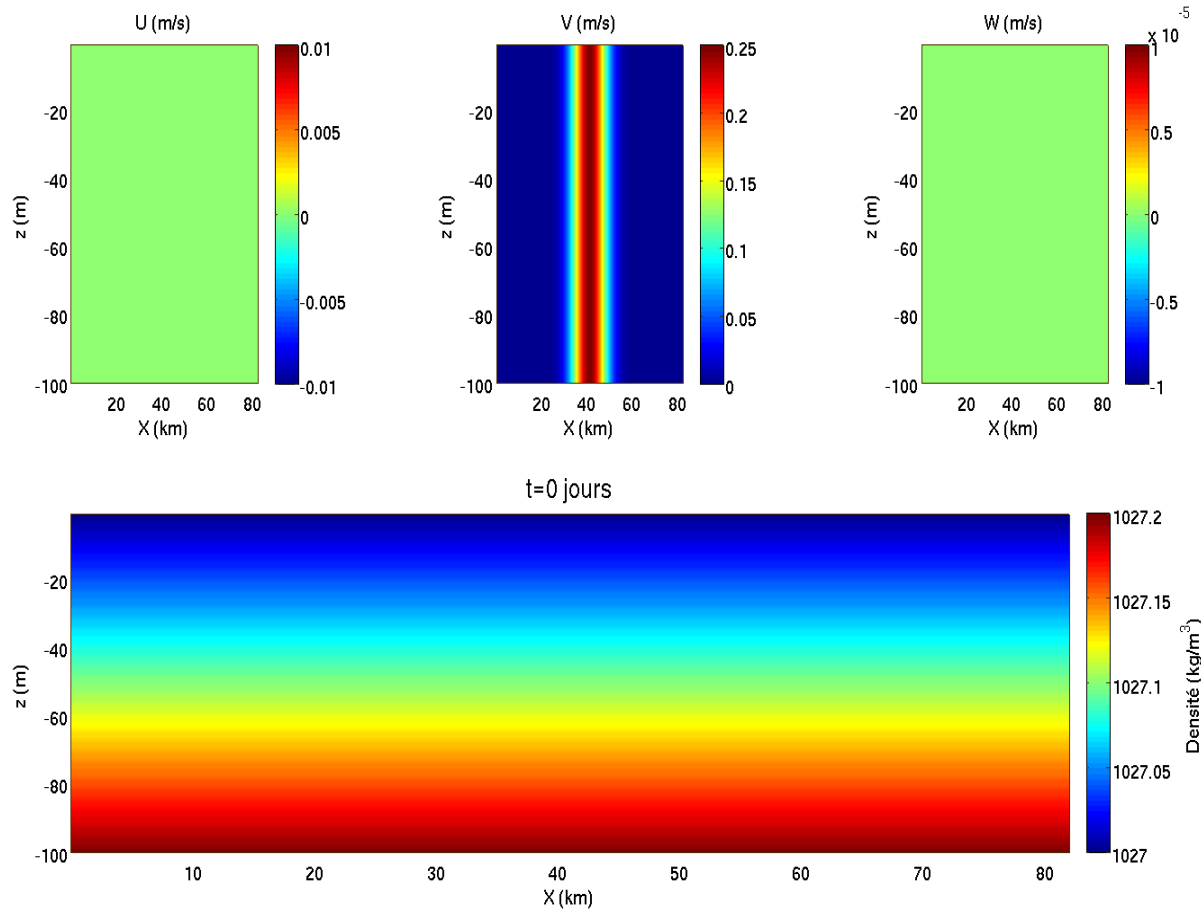
- Let's consider a barotropic jet on a coastal ocean with constant depth.
- There is an Ekman layer on the bottom.
- The vertical gradient of density is weak.



Non-hydrostatic idealized model

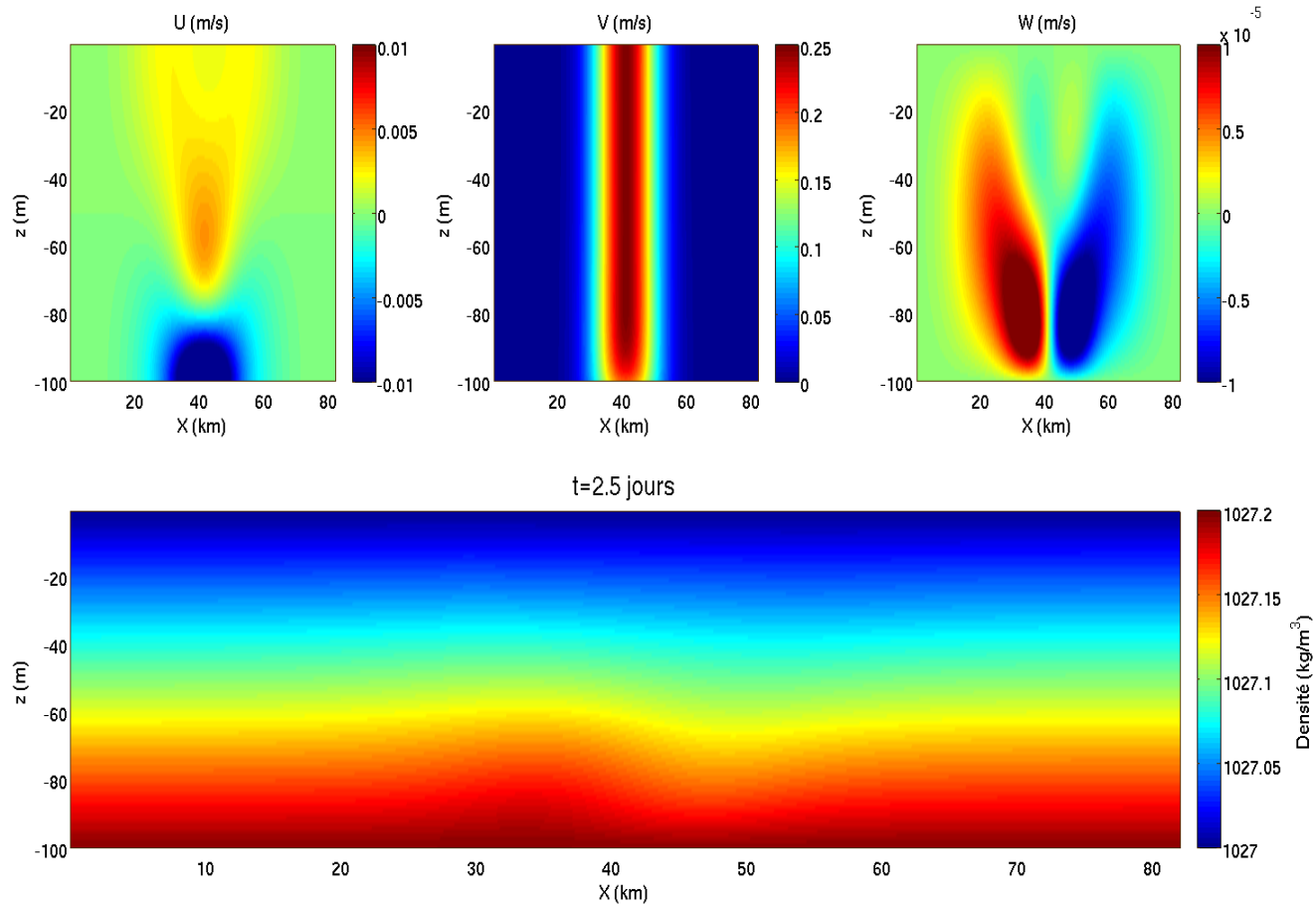
- Model parameters:
 - Meshing
 - 1024*80 m in the x direction
 - 100*1 m in the z direction
 - Non-hydrostatic simulation
- Physical parameters
 - $H=100$ m
 - $V_0=0,25$ m/s
 - $\nu_v=5 \cdot 10^{-2}$ m/s⁻²

Model results



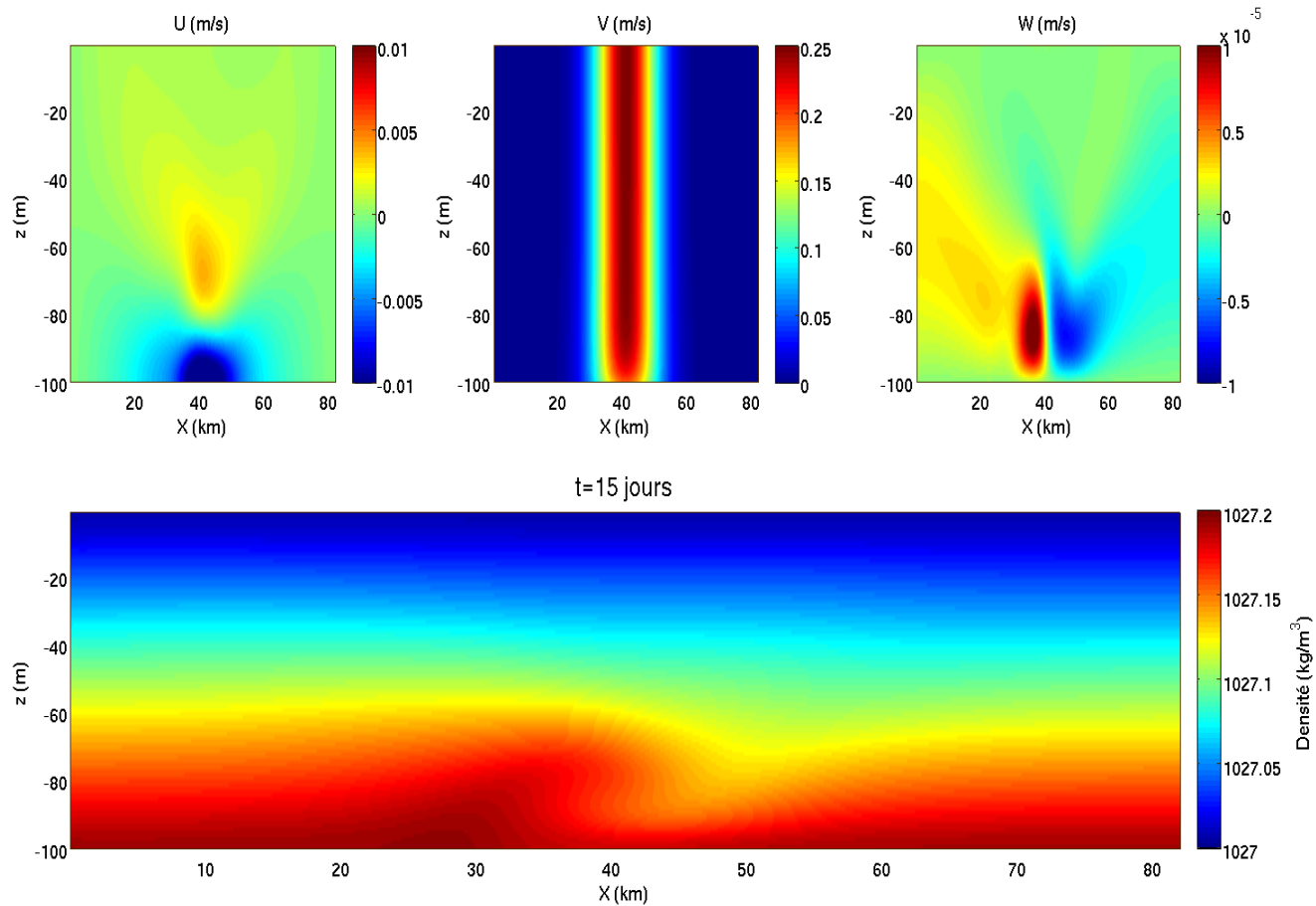
Initial conditions

Model results



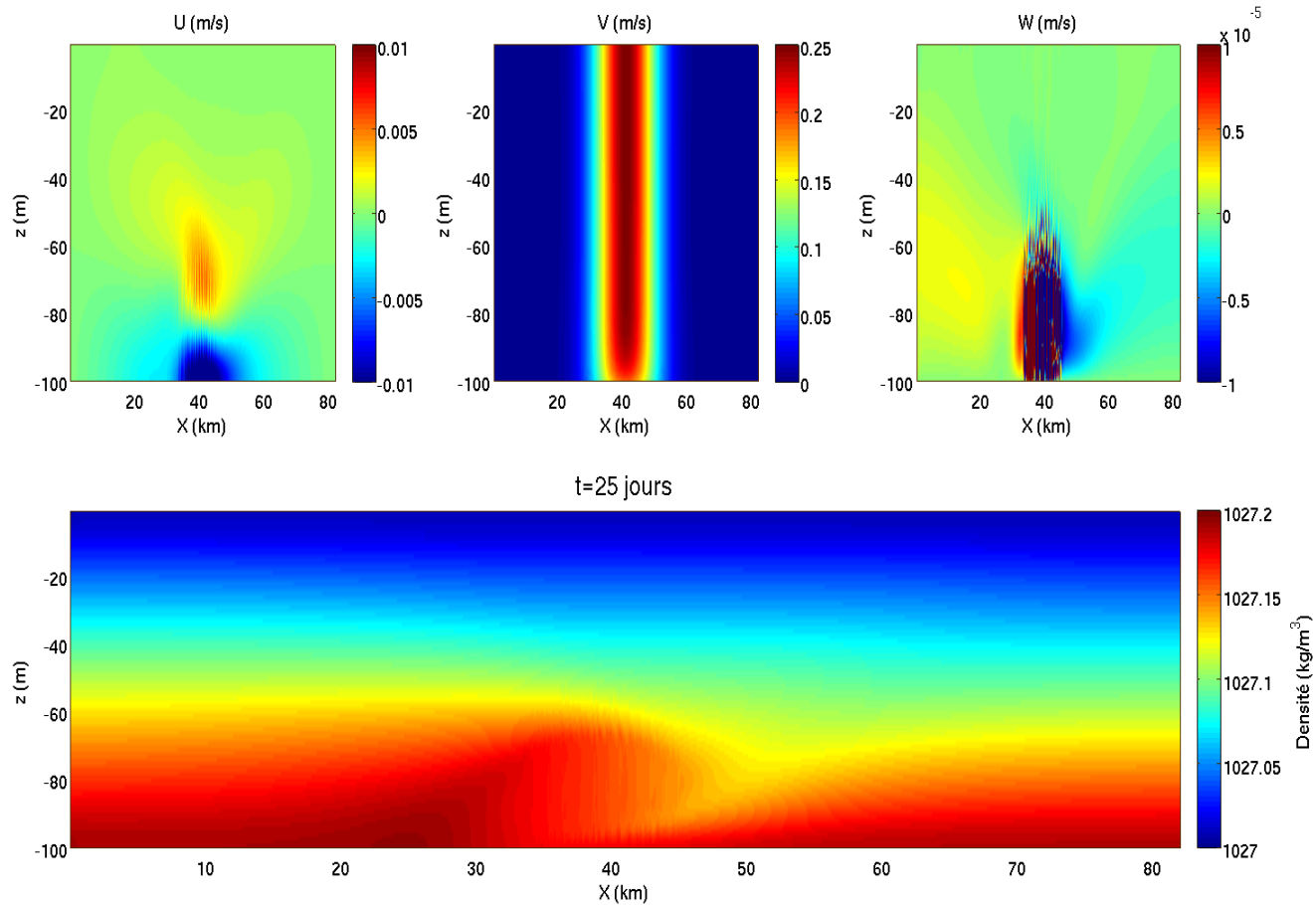
1st step: set up of the Ekman layer

Model results



2nd step: advection of the density field

Model results



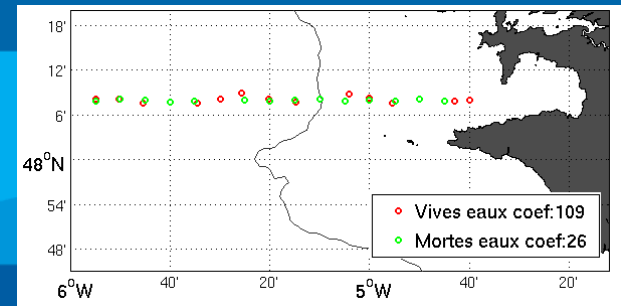
3rd step: convection

Animation

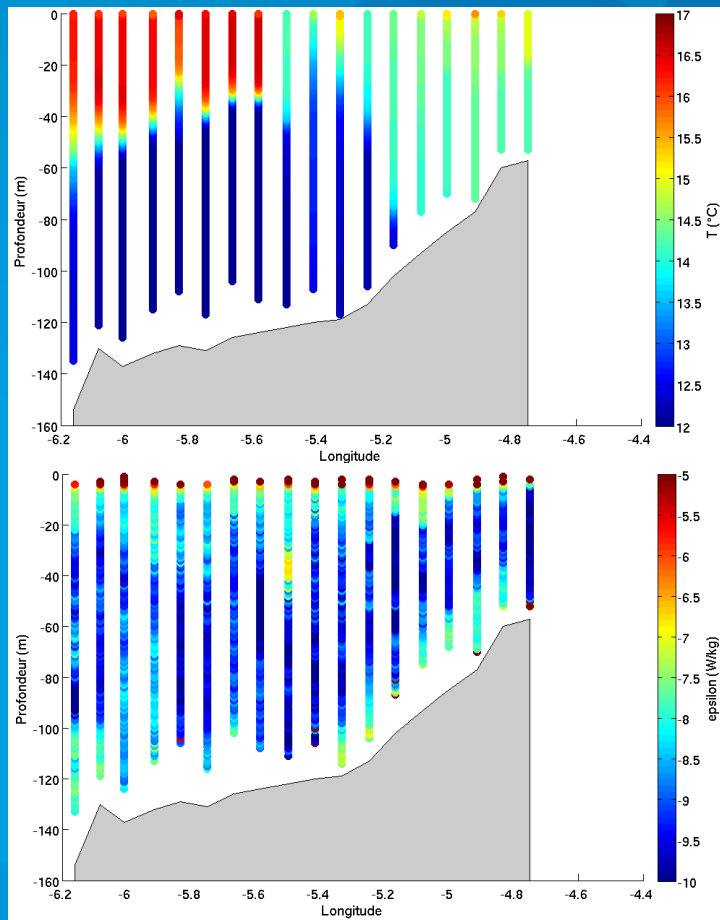


VMP measurement

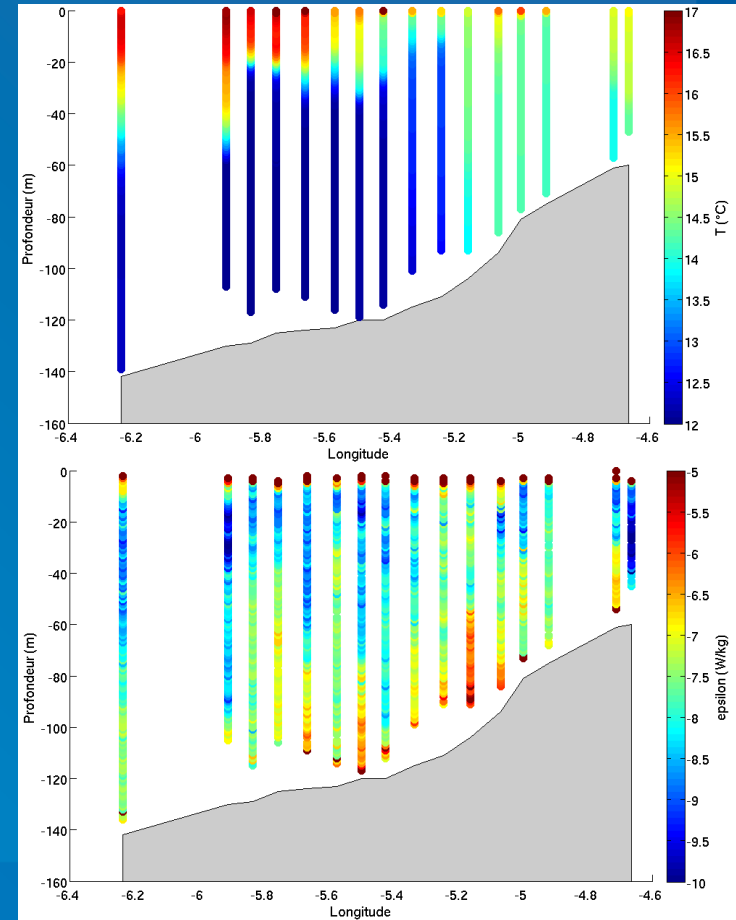
Observations made during the FROMVAR 2009 cruise,
(coll. Bruno FERRON)



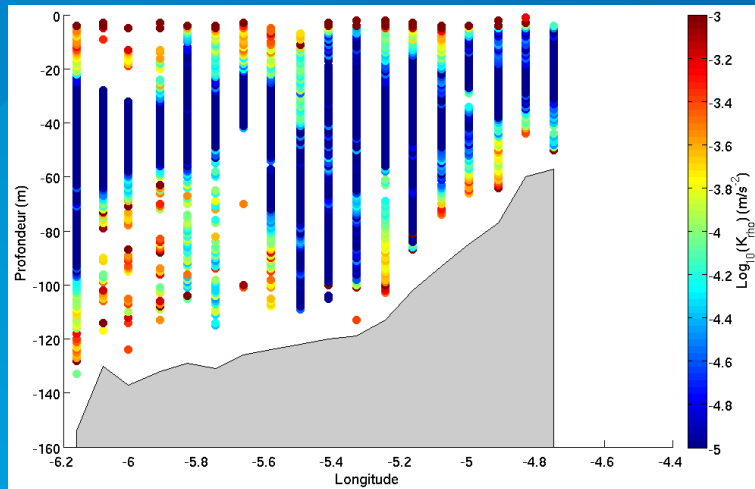
Neap



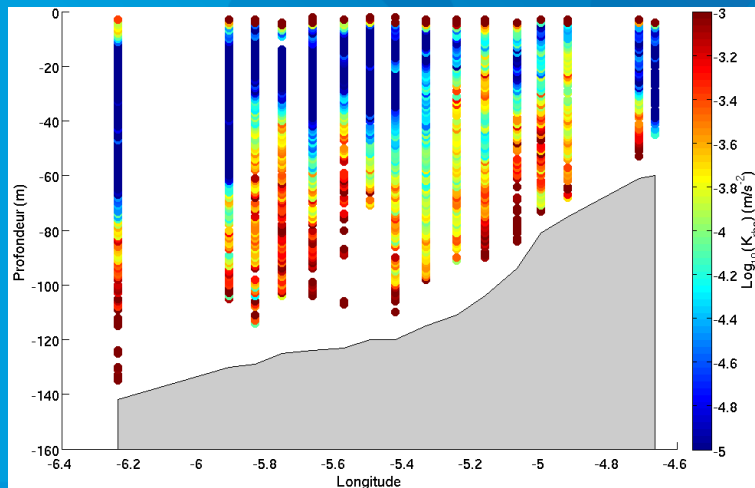
Spring



VMP measurement



Neap



Spring

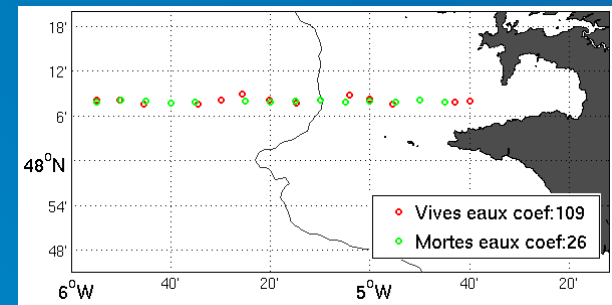
Parametrisation of scalar eddy diffusivity by Shih et al. 2005

For $\epsilon/\nu N^2 < 100$

$$\kappa_{\rho} \sim 0,2\epsilon/N^2$$

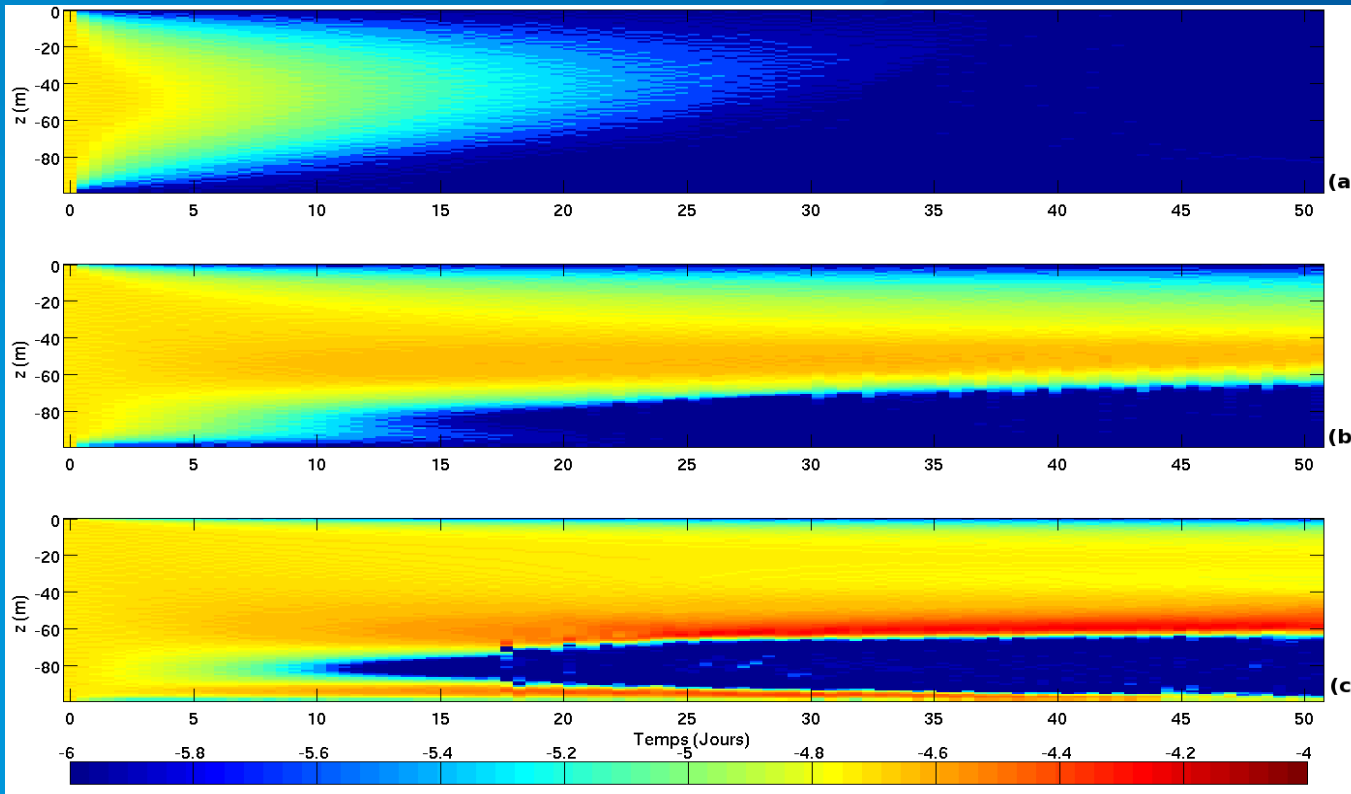
For $\epsilon/\nu N^2 > 100$

$$\kappa_{\rho} \sim 2\nu(\epsilon/\nu N^2)^{1/2}$$



Sensibility to the diffusion parameter

Vertical section of $\log_{10}(N^2)$ vs time at $x=40\text{km}$

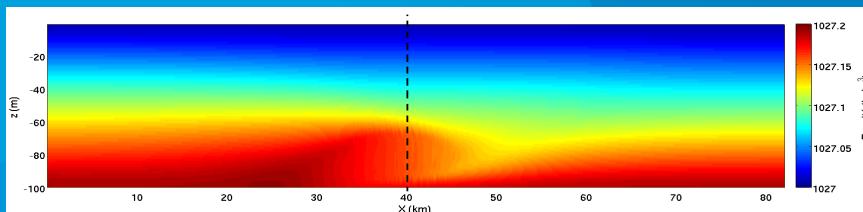


Evolution of the Brunt-Väisälä frequency for

(a) $\kappa_{\rho} = 10^{-3} \text{ m/s}^2$

(b) $\kappa_{\rho} = 10^{-4} \text{ m/s}^2$

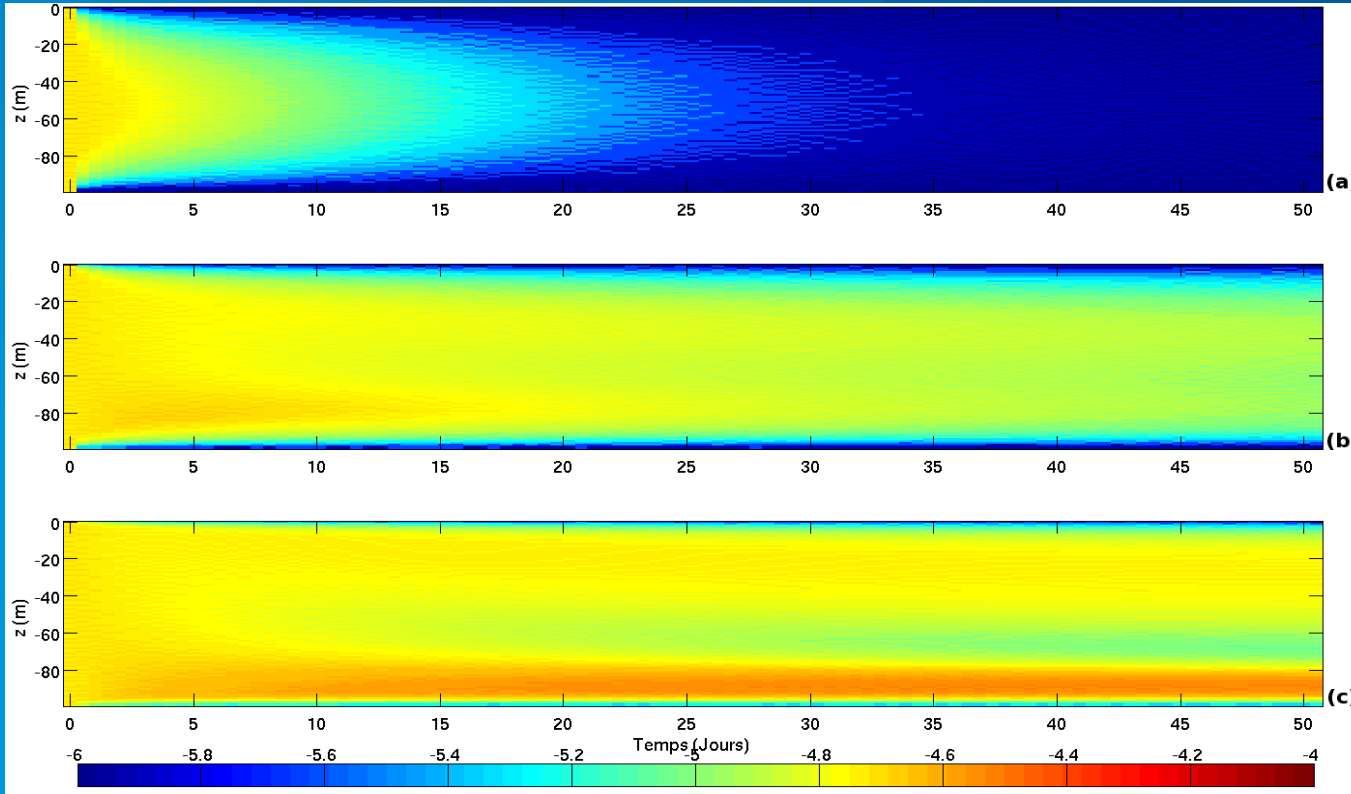
(c) $\kappa_{\rho} = 10^{-5} \text{ m/s}^2$



Position of the vertical section

Sensibility to the diffusion parameter

Vertical section of $\log_{10}(N^2)$ vs time at $x=55\text{km}$

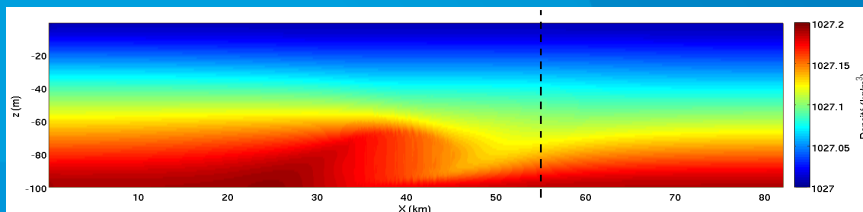


Evolution of the Brunt-Väisälä frequency for

(a) $\kappa_{\rho} = 10^{-3} \text{ m/s}^2$

(b) $\kappa_{\rho} = 10^{-4} \text{ m/s}^2$

(c) $\kappa_{\rho} = 10^{-5} \text{ m/s}^2$



Position of the vertical section

Conclusion

- The residual circulation observed in the Iroise sea may be involved in the dynamics of the Ushant front.
- The divergence of the Ekman transport can homogenize the water column on the right side of the jet and stratify on the left.
- This mechanism may play a role in the formation of the Ushant front.

Perspectives

- A better model is needed to represent the space-time variation of the diffusion.
- Is this mechanism involved in the spring-neap variation of the front?